Investigations of the middle atmospheric thermal structure and oscillations over sub-tropical regions in the Northern and Southern Hemispheres

Som Sharma, Prashant Kumar, Chintan Jethva, Rajesh Vaishnav, Hassan Bencherif

Investigations of the middle atmospheric thermal structure and oscillations over sub-tropical regions in the Northern and Southern Hemispheres

Som Sharma[1] · Prashant Kumar[2] · Chintan Jethva[1,3] · Rajesh Vaishnav[1] · Hassan Bencherif[4]

Abstract The temperature retrieved from the Sounding of the Atmosphere using Broadband Emission Radiometry (SABER) onboard Thermosphere Ionosphere Mesosphere Energetics and Dynamics (TIMED) satellite during January 2002 to September 2015 are used in this study to delineate the differences of middle atmospheric thermal structure in the Northern Hemisphere (NH) and Southern Hemisphere (SH). Two stations namely Mt. Abu (24.59°N, 72.70°E) in NH and Reunion Island (21.11°S, 55.53°E) in SH are chosen over sub-tropical regions. Temperature climatology from SABER observations suggests that stratopause is warmer, and upper mesosphere is cooler in NH as compared to SH. Three atmospheric models are used to understand the monthly thermal structure differences for different altitudes. Moreover, semi-annual, annual and quasi-biennial oscillations are studied using Lomb Scargle Periodogram and Wavelet transform techniques. Over NH, summer and winter season are warmer (~4 K) and cooler (~3 K) respectively in stratosphere as compared to SH. It is important to note here that Mt. Abu temperature is warmer (~9 K) than Reunion Island in winter but in summer season Mt. Abu temperature is cooler in upper mesosphere and above mesosphere NH shows warming. Results show that annual oscillations are dominated in both hemisphere as compared to semi-annual and quasi-biennial oscillations. In upper mesosphere, strength of annual oscillations is substantial in NH, while semi-annual oscillations are stronger in SH. Wavelet analyses found that annual oscillations are significant in NH near mesopause, while semi-annual oscillations are strengthening in SH.

Keywords Atmospheric dynamics · Middle Atmosphere · SABER · Atmospheric models

✉ Som Sharma
somkumar@prl.res.in

1 Physical Research Laboratory, Ahmedabad 380009, India

2 Space Applications Center (ISRO), Ahmedabad 380015, India

3 Dept. of Physics, Saurashtra University, Rajkot, India

4 Laboratory of the Atmosphere and Cyclones, LACY, Reunion, France

1 Introduction

Northern Hemisphere (NH) and Southern Hemisphere (SH) have varying and diverse geophysical processes due to differences in land cover, ocean extents, radiative fluxes, etc. NH has about 90 % of the population while SH has large oceanic region. Due to lesser human existence in the SH, studies of the Earth's atmosphere are relatively less in general, and in particular, middle atmospheric studies are sparser as it is rather difficult to probe middle atmosphere from ground based instruments. Thermal structure is one of the efficient approach to understand inter-hemispheric coupling of the middle atmosphere. Kornich and Becker (2010) found that anomalous stratospheric and mesospheric features are due to residual circulation pattern. To enhance our scientific understanding of the middle atmosphere, it is crucial to compare the NH and SH processes using similar kind of observations from various observing platforms and numerical models.

Hauchecorne et al. (1991) were the first to establish middle atmospheric temperature climatology using Rayleigh Lidar observations from two stations in France. Later, Gobbi et al. (1995) presented a mid-latitude temperature variability over Frascati (42°N, 13.6° E). Temperature climatology of the middle atmosphere (from ~30 to

~90 km) have been studied by several groups (e.g., Barnett and Corney 1985; Chanin et al. 1985; Jenkins et al. 1987; Hauchecorne et al. 1991; Clancy et al. 1994; Whiteway and Carswell 1994; Leblanc et al. 1998; Bencherif et al. 2000; Gardner et al. 2001; Nee et al. 2002; Sivakumar et al. 2003; Randel et al. 2004; Argall and Sica 2007; Gerding et al. 2008; Li et al. 2008; Batista et al. 2008, 2009; Kishore Kumar et al. 2008; Dou et al. 2009, Sivakumar et al. 2011; Sharma et al. 2006, 2012, 2015). Thermodynamic profiles from troposphere to mesosphere were studied by various groups using Lidars (e.g., Hauchecorne et al. 1992; Gross et al. 1997 and reference therein). Namboothiri et al. (1999) compared satellite retrieved temperature profiles and CIRA-86 (COSPAR International Reference Atmosphere) model with Lidar and Rocket measured profiles and found that the Lidar temperatures are agreeing well with rocket and satellite borne measurements. Ground based Lidar measured temperatures were also used for the validation of several remote sensing instruments e.g. Microwave Limb Sounder (MLS), HALOE (Halogen Occultation Experiment) onboard UARS (e.g., Remsberg et al. 2002; Cooper 2004, Sica et al. 2008 and references therein). Over the Indian tropical latitudes in NH, thermal structure was studied initially from rocket borne observations (Sasi and Sengupta 1979; Lal et al. 1979; Sasi 1994; Mohankumar 1994) and later using ground based Lidar measurements (e.g., Parameswaran et al. 2000; Sivakumar et al. 2003; Chandra et al. 2005; Sharma et al. 2006, 2012, 2015). A study using 14 years of Lidar data on the seasonal thermal amplitude were reported by Batista et al. (2009) at Sao Jose dos Campos, Brazil (23°S, 46°W) in the SH and found significant differences in the temperatures simulated from the atmospheric model. Another Lidar based study of middle atmospheric thermal structure in the SH at Reunion Island (21.11°S, 55.53°E) was presented by Sivakumar et al. (2011). They reported that the Lidar observed profiles are in qualitative agreement with the satellite observations. In addition, few studies are available in SH covering low latitudes and sub-tropics (e.g., Bencherif et al. 2000; Morel et al. 2002; Batista et al. 2008, 2009). Vertical profiles of temperature are also available from HALOE onboard UARS (1992–2005), COSMIC (Constellation Observing System for Meteorology, Ionosphere, and Climate) and other GPSRO (Global Positioning System Radio Occultation) mission, hyperspectral infrared sounder on board AQUA, and SABER (Sounding of the Atmosphere using Broadband Emission Radiometry) onboard TIMED (Thermosphere Ionosphere Mesosphere Energetics and Dynamics). Simultaneous observations in the stratosphere and mesosphere from these instruments have further provided a platform to study the coupling between different regions and this further lead to improved skill of model predictions.

Gravity waves (GW) and planetary waves (PW) characteristics are highly varying regionally and seasonally over the globe, and have significant differences in the NH and SH (Fritts and Vanzandt 1993; Fritts and Alexander 2003). Waves of non-orographic origin modulate winds at mesospheric heights, and even affect total stratosphere in the tropical and sub-tropical regions, and are one of the major drivers of the Quasi Biennial Oscillations (QBO) and Semi-Annual Oscillations (SAO) (e.g., Alexander and Rosenlof 1996; Baldwin et al. 2001; Giorgetta et al. 2002; Pulido and Thuburn 2008; Sato et al. 2009 and reference therein). The SAO are also playing a vital role in deciding overall dynamics of the Earth's atmosphere (Garcia et al. 1997). Features of stratospheric stationary planetary waves (SPW) in the NH and SH was presented by various authors (e.g., Hirota et al. 1983; Hartmann et al. 1984; Mechoso et al. 1985; Shiotani and Hirota 1985; Andrews 1989). Forbes et al. (2002) reported PW structures and their seasonal variability in the altitude range of 15–100 km using data from High Resolution Doppler Imager (HRDI) and Wind Imaging Interferometer (WINDII) onboard Upper Atmosphere Research Satellite (UARS). Gray et al. (2010) reported impact of QBO on middle atmospheric temperature and dynamics. During winter in the NH, easterly phase of QBO is responsible for poleward as well as downward propagating easterly wind anomalies (Matthes et al. 2013).

Latitudinal coupling is another very pertinent aspect for the study of atmospheric system in whole. Tropical and sub-tropical regions are very much prone to be influenced by different hemispheres as being close to the equator. Stronger equatorial processes in either of the hemispheres modulates each other. Therefore, it is very much needed to explore different atmospheric regions of the NH and SH to quantify the similarities, differences and anomalies in the tropical and sub-tropical regions of the different hemispheres. Present study is focussed on the middle atmospheric thermal structures and characteristics of SAO, AO (Annual Oscillations) and QBO over two regions, Mt. Abu in the NH, and Reunion Island almost at similar latitude in the SH, using SABER onboard TIMED satellite during January 2002 to September 2015. Similarities and differences in thermal fields and oscillations have been extensively analysed, and findings are discussed using Lomb–Scargle Periodogram, and to further delineate the presence of SAO, AO and QBO using wavelet techniques.

2 Instrumentation and data

In this paper, we have used observations from SABER onboard TIMED satellite from January 2002 to September 2015 over Mt. Abu, a subtropical location in the NH, and over Reunion Island which is located in the sub-tropics

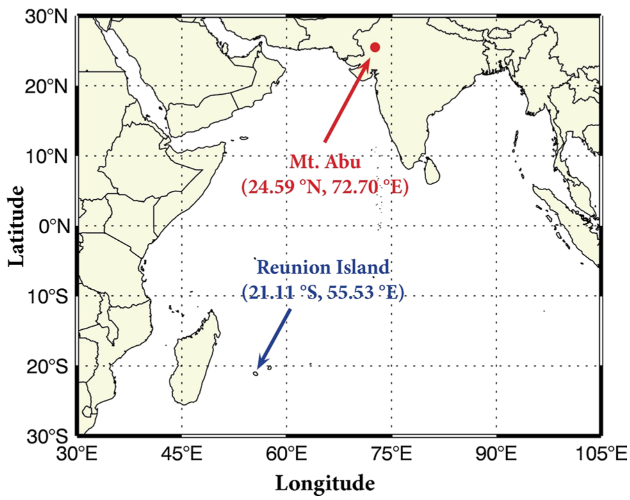

Fig. 1 Geographic locations of the study regions

of the SH (Fig. 1). Radiometric technique have been exploited effectively to retrieve vertical temperature profiles in SABER. It measures radiations from 1.27 to 17 μm covering ten spectral channels in limb direction. The temperature in the stratosphere-mesosphere-lower thermosphere is retrieved from atmospheric CO_2 emission at 15 μm (Mertens et al. 2001, 2009). The SABER on-board TIMED satellite covers 15 orbits in a day at an altitude of about 625 km having an orbital inclination of 74.1° to the equator. Mertens et al. (2001) and Remsberg et al. (2008) presented an extensive study on the observational and retrieval errors in the SABER observed temperatures. Mertens et al. (2001) reported uncertainty in the retrieval and found that it is about 1.4 K at 80 km and 22.5 K at 110 km. The SABER measurements have been used in the 5° × 5° latitude-longitude grid, centred over Mt. Abu and Reunion.

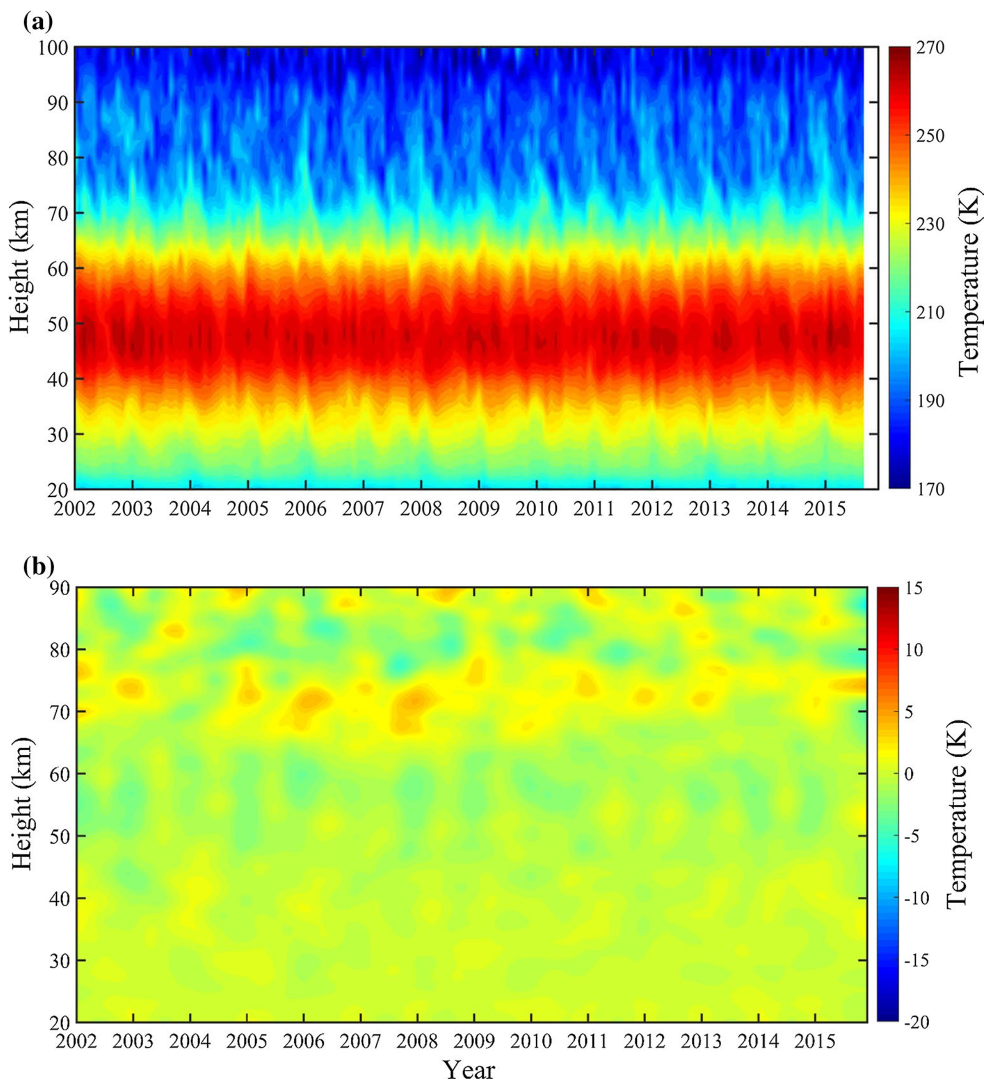

Fig. 2 Temporal variation of **a** SABER retrieved temperature observations and **b** moving annual average temperature difference between Mt. Abu and Reunion Island during January 2002 to September 2015

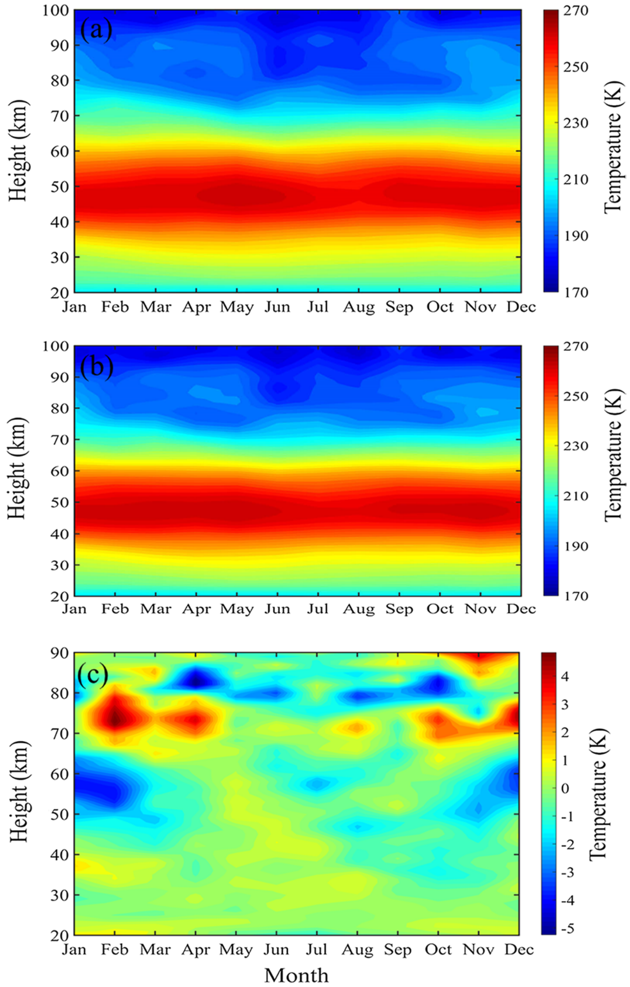

Fig. 3 Monthly temperature climatology from SABER onboard TIMED satellite over **a** Mt. Abu and **b** Reunion Island. **c** Monthly temperature difference between Mt. Abu and Reunion Island

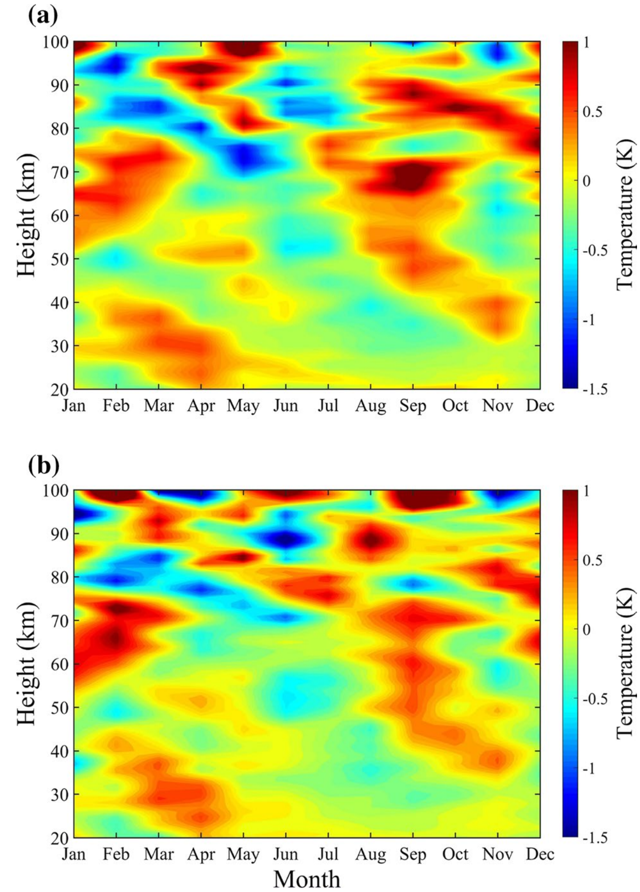

Fig. 4 Monthly temperature anomaly using SABER observations over **a** Mt. Abu and **b** Reunion Island

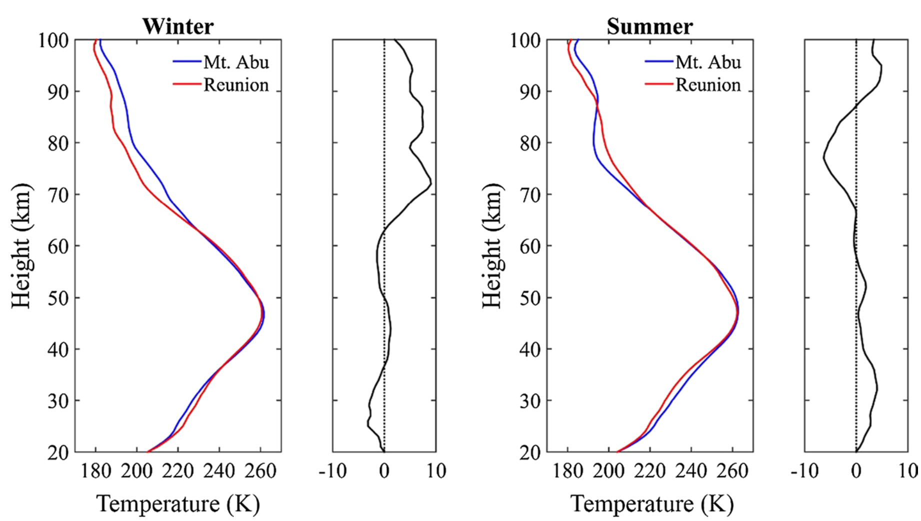

Fig. 5 Thermal structure of Mt. Abu and Reunion Island in winter and summer seasons. Differences between Mt. Abu and Reunion Island temperature are also shown in *right panels*

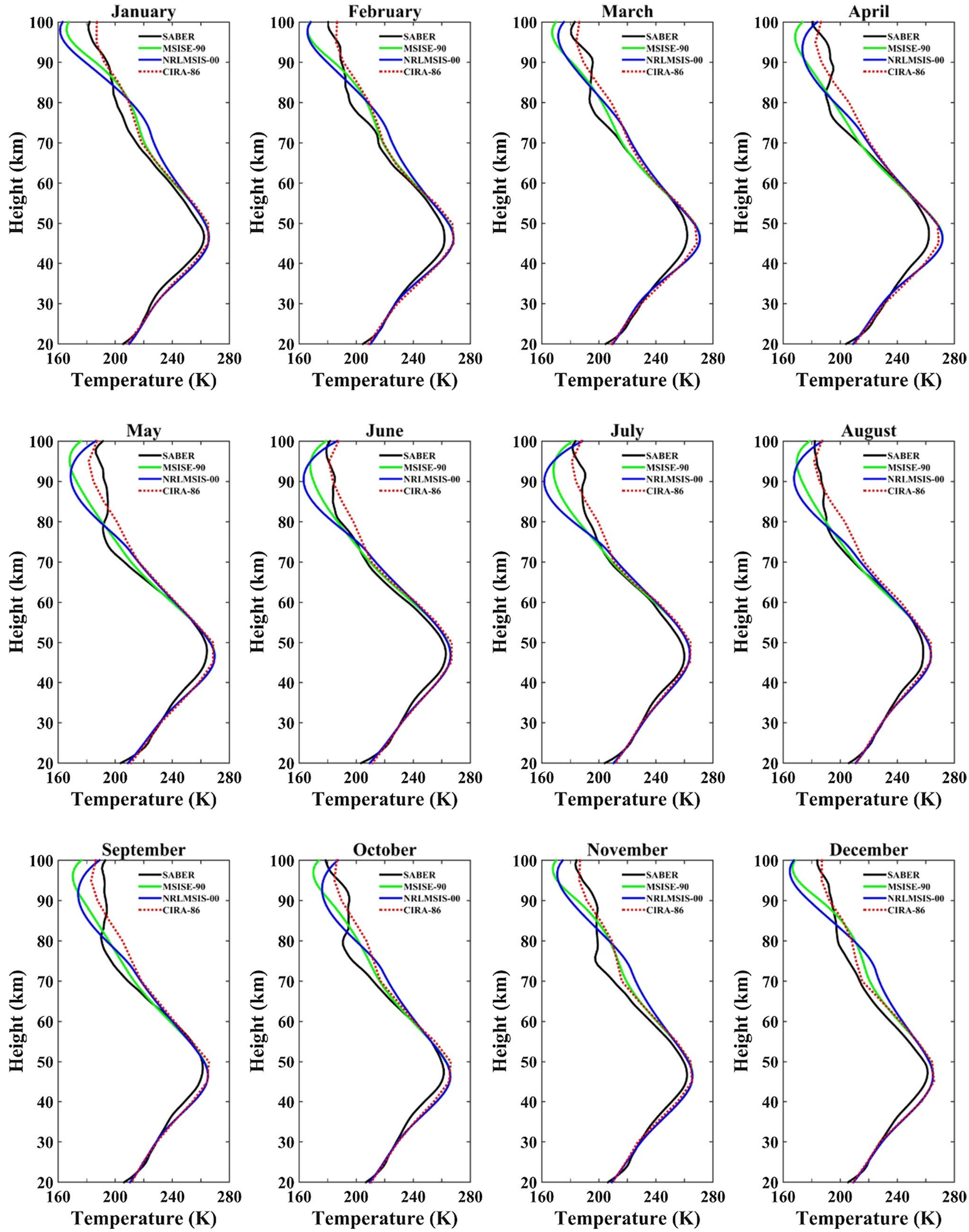

Fig. 6 Monthly temperature profile from SABER and CIRA-86, MSISE-90 and NRLMSISE-00 empirical models over Mt. Abu

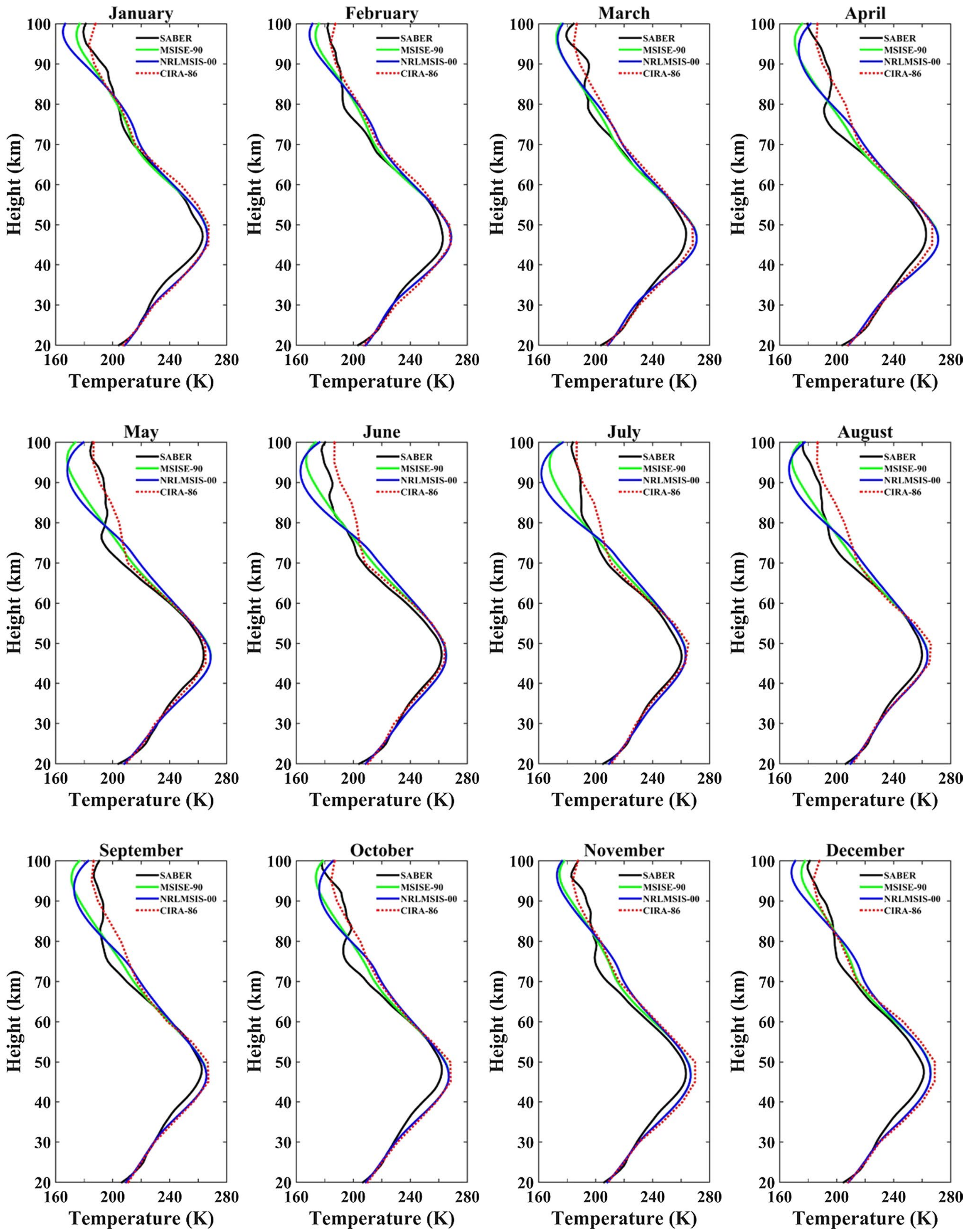

Fig. 7 Same as Fig. 6 but for Reunion Island

Table 1 SABER observed and atmospheric models simulated temperature over Mt. Abu

Altitude (km)	SABER (K)	MSIS (K)	NRLMSIS (K)	CIRA (K)	SABER-MSISE (K)	SABER-NRLMSIS (K)	SABER-CIRA (K)
20.0	205.2	209.7	209.7	210.2	−4.5	−4.5	−5.0
30.0	229.1	229.5	229.5	229.5	−0.3	−0.3	−0.4
40.0	250.8	256.8	256.9	256.0	−6.0	−6.2	−5.2
50.0	259.9	264.2	263.8	266.0	−4.4	−3.9	−6.1
60.0	238.6	239.8	241.8	241.3	−1.2	−3.2	−2.7
70.0	211.3	215.0	220.5	216.8	−3.7	−9.2	−5.5
80.0	193.7	198.6	197.7	205.5	−4.9	−3.9	−11.7
90.0	192.3	178.7	173.8	188.2	13.6	18.5	4.1
100.0	183.7	173.5	179.8	186.9	10.3	3.9	−3.1

Table 2 SABER observed and atmospheric models simulated temperature over Reunion Island

Altitude (km)	SABER (K)	MSIS (K)	NRLMSIS (K)	CIRA (K)	SABER-MSISE (K)	SABER-NRLMSIS (K)	SABER-CIRA (K)
20.0	205.0	208.7	208.7	209.1	−3.7	−3.7	−4.1
30.0	229.2	229.7	229.7	229.7	−0.5	−0.5	−0.5
40.0	250.8	257.1	257.2	256.7	−6.3	−6.4	−5.9
50.0	260.7	264.9	264.6	267.0	−4.2	−3.9	−6.3
60.0	239.8	240.6	242.2	242.4	−0.8	−2.4	−2.6
70.0	210.2	214.6	219.0	214.9	−4.4	−8.8	−4.7
80.0	195.1	197.1	197.4	204.3	−2.0	−2.2	−9.2
90.0	191.4	178.3	174.4	189.1	13.2	17.0	2.3
100.0	182.7	176.1	176.9	187.0	6.6	5.7	−4.3

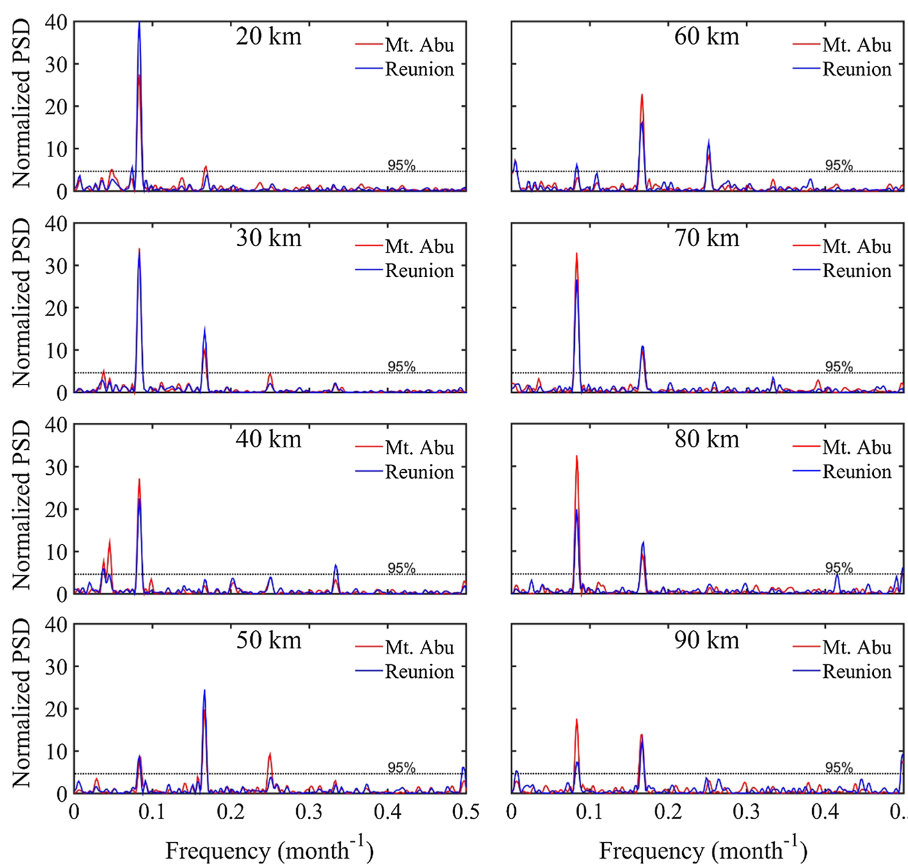

Fig. 8 Lomb Scargle periodogram for SABER retrieved temperature at every 10 km. The *black dotted line* shows significant changes at 95 % confidence interval

3 Results and discussion

3.1 Temporal variations

The aim of this study is to understand the characteristics of sub-tropical middle atmosphere in NH and SH. To understand the behaviour of stratosphere-mesosphere thermal structure in two different hemispheres, SABER onboard TIMED satellite observations are used in this study from 20 to 100 km vertically during January 2002 to September 2015. Temporal variation of SABER retrieved monthly mean temperature during study period for Reunion station is shown in Fig. 2a, and the moving annual average temperature difference between Mt. Abu and Reunion temperature observations is depicted in Fig. 2b. As compared to Mt. Abu, stratopause temperature (at ~47 km) is relatively less (~2 K) in Reunion Island, which can be easily detected from Fig. 2b. It is interesting to note that Mt. Abu temperatures are higher than Reunion temperatures above 70–80 km. These differences reach up to larger than 5 K. In general, mean climatological behaviour of upper mesosphere shows that NH has higher temperature as compared to SH. Kang et al. (2013) used surface temperature data and re-investigated Croll's 140-year-old theory (Croll 1870) that NH is warmer than SH due to northward cross-equatorial ocean heat transport. This may be due to a transient response of greenhouse gas forcing because the NH has larger land regions which warm faster than oceanic region (Philander et al. 1996; Kang et al. 2013). The different characteristics of lower tropospheric temperature affect the Gravity waves, which influences subsequently to middle atmosphere. Fritts (1990) studied that both hemispheres reveal similar Gravity waves characteristics in lower and middle atmosphere mainly in case of scales, growth of amplitude with height. However, significant differences were found by authors in the wave spectra and their influences in different hemispheres. Gravity waves transport momentum from lower atmosphere to upward direction (e.g., Fritts and Alexander 2003; Sato et al. 2012). Becker et al. (2004) found inter-hemispheric coupling of the middle atmospheric circulations in a case study. Kornich and Becker (2010) also discussed the inter-hemispheric coupling and essential steps of this coupling were presented in details by Karlsson et al. (2009). In mesosphere at 70–80 km, Fig. 2b shows that temperature is higher in NH against SH.

Monthly climatology is prepared using SABER retrieved temperature profiles from 14 years of observations. Figure 3 shows that higher than 250 K temperature is observed at stratopause region over Mt. Abu as well as over Reunion Island. The NH (Fig. 3a) shows maximum warming in April and May months (~265 K), this higher temperature values are not found in Reunion Island (Fig. 3b). Mt. Abu region shows cooler temperature in upper mesosphere during winter season (November to January) over NH. This cold temperature reaches up to 90 km altitude. In contrary to these changes in the NH, the SH also shows cooler temperature in the months of June and July. The difference between Mt. Abu and Reunion temperature (Fig. 3c) shows that higher temperature is found in upper mesosphere except May to September months. Cooler temperature is seen in mesopause over SH during April to October months. Moreover, high temperature is found in lower mesosphere in NH compared to SH during November to February months. In general, stratosphere shows higher temperature at Mt. Abu compared to Reunion Island (Fig. 3c).

Climatology of monthly temperature anomaly, defined as difference between mean monthly temperature (e.g. average values of January for all years) minus mean annual temperature, is prepared using SABER observations. Figure 4a, b shows the temperature anomaly for Mt. Abu and Reunion Island respectively for stratosphere-mesosphere system. Both hemispheres show similar temperature structure in stratosphere, which are higher during February to April and November months and marginally less in the months of August. Somewhat positive anomaly is found in the SH as compared to the NH in the months of December to February (winter period in the NH) within 50–70 km. These anomalies are reverse in nature during August and September months, represents positive value of anomaly in Mt. Abu as compared to Reunion Island. The NH (Fig. 4a) shows coolest temperature at ~85 km in the months of February, and this cooling is shifted at lower altitude from February to September months, which followed by a warmer anomaly trend. Almost similar features are visible in the SH at Reunion Island.

To understand the seasonal variation (e.g. winter, summer season) in both hemisphere, mean temperature during winter and summer for Mt. Abu and Reunion Island and their differences are shown in Fig. 5. Winter and summer season used in this study are December–January–February and June–July–August months respectively in NH. For SH, June–July–August and December–January–February months are selected as winter and summer period respectively. During winter season, stratosphere is cooler over Mt. Abu. At stratopause, both stations show nearly same mean temperature, and in upper mesosphere Mt. Abu is warmer than Reunion Island. In summer season, Mt. Abu shows slightly higher temperature in stratosphere. Above this

Fig. 9 A continuous Wavelet transform of the temperature retrieved ▶ from SABER satellite representing temporal variations of frequency at every 10 km altitude over Mt. Abu region. A time series of temperature at same altitude during January 2002 to September 2015 is shown in *lower panel*. *Black line* in the contour plot shows cone of confidence. *Line plot* of power and confidence interval at all altitudes are also shown in the *right side panel* of each contour plot

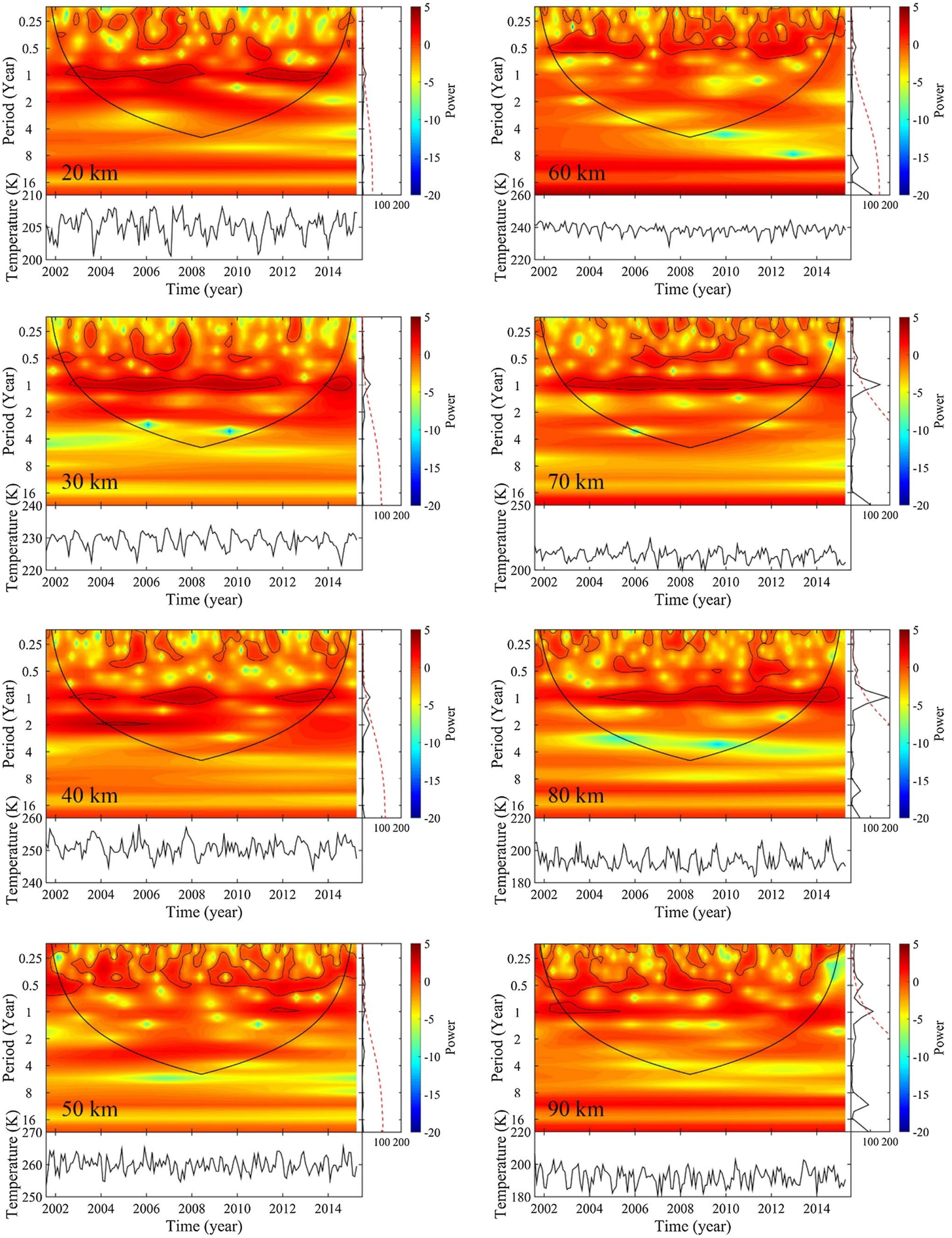
20 km
30 km
40 km
50 km
60 km
70 km
80 km
90 km
Period (Year)
Temperature (K)
Time (year)
Power
0.25
0.5
1
2
4
8
16
100 200
5
0
-5
-10
-15
-20
2002
2004
2006
2008
2010
2012
2014

altitude, Mt. Abu shows cooler temperature within ~67 to 87 km, and further shows more warming as compared to Reunion Island. These results show that the NH is warmer and cooler in summer and winter season respectively as compared to SH in stratosphere, and opposite nature is found in upper mesosphere. This diverse nature may be due to large landmass and high low level warming in the NH.

Figure 5 shows that both the hemispheres have systematic changes in middle atmosphere during two different seasons. This finding motivate us to further investigate the monthly variation of thermal structure. In addition to SABER observations, three different atmospheric models named as CIRA-86, Mass Spectrometer and Incoherent Scatter Radar Extended (MSISE-90) and Naval Research Laboratory Mass Spectrometer and Incoherent Scatter Radar (NRLMSIS-00) are used to evaluate the thermal structure of atmospheric models. Figures 6 and 7 show the monthly mean temperature for Mt. Abu and Reunion Island respectively. To calculate monthly temperature, SABER observations and model simulations are used during year 2002 to 2015. Figures 6 and 7 show that model's simulated temperature profiles are in good agreement with SABER observations in both hemispheres up to ~30 km. The possible reason may be that various atmospheric sounder in microwave and infrared frequency are available from last few decades which provide temperature and moisture profiles, and very accurate in nature up to ~30 km. These satellite observations are used directly or indirectly in atmospheric models because of that quality of temperature sounding is improved a lot in troposphere and lower stratosphere. At upper stratosphere, slightly higher value of temperature are simulated from atmospheric models as compared to temperature observed from SABER. These differences are maximum in the months of March and April over Mt. Abu region (Fig. 6) and minimum in the months of November. Over Reunion Island, minimum changes are found in the month of June and these changes are higher in March, April and December months. It is interesting to note here that at these vertical levels, all selected atmospheric models show similar kind of warming in the NH, and no significant differences are found in monthly variations. But in case of SH, CIRA-86 model perform better in winter period compared to other two atmospheric models, and worse in summer season at upper stratosphere. In the upper mesosphere around 60 to 80 km, SABER shows minimum temperature for all months over different hemisphere. The differences between atmospheric model's simulations and SABER observations are very high in the months of January, February, and October to December (mainly winter period in NH). These differences are minimum during June to August months for same altitude. In contrary to these results in the NH, the SH (Fig. 7) shows less difference in model simulations and SABER observations at upper mesosphere (~60–80 km) except April, May and September to October months. Overall, we found that somewhat cooler temperature is seen in NH as compared to SH in upper mesosphere. In mesopause region, MSISE-90 and NRLMSIS-00 models are not able to capture temperature accurately for all months over the NH and SH, both models show similar kind of under-estimation at this altitude. But, CIRA-86 model simulated temperature values are close to SABER observations. Slightly more skill is found in the SH as compared to NH temperature at this altitude in the months of January and February. Tables 1 and 2 show the SABER observed and model simulated temperature at every 10 km start from 20 to 100 km. Table shows that Reunion Island has minutely higher (~2 K) temperature at 80 km in comparison to Mt. Abu. Maximum error in atmospheric models can be seen at high altitude, which is relatively higher in the NH (Table 1) as compared to the SH (Table 2). In both hemispheres, slightly higher (~4 K) and lesser (~8 K) temperature are simulated from models at 20 and 90 km respectively. Temperature simulated from CIRA-86 is significantly less at 90 km as compared to MSISE-90 and NRLMSIS-00 atmospheric model in both hemispheres. Batista et al. (2009) also studied the seasonal thermal amplitude using 14 years of Lidar measurements and found noticeable differences in the temperatures observed from the MSISE-90 model. Similar kind of comparison are also found in this study when model temperature profiles are compared with SABER observations.

3.2 Characteristics of annual, semi-annual and quasi-biennial oscillations

To understand the nature of oscillations in NH and SH, the Lomb Scargle periodogram (LSP; Scargle 1982; Lomb 1976; Sivakumar et al. 2011) and Wavelet transform (Farge 1992; Das and Sinha 2008) techniques are used for SABER observations during year 2002–2015 in the stratosphere-mesosphere system. This study will help to distinguish the wave dynamics or wave features of the middle atmospheric region. Previously, Sivakumar et al. (2011) used LSP to study seasonal oscillations from Lidar observations over Reunion Island. The objective of this study is to establish resemblances and alterations over the NH and SH.

Figure 8 shows the different oscillations viz. semi-annual (SAO), annual (AO) and quasi-biennial (QBO) oscillations at every 10 km start from 20 to 90 km for both locations selected in the NH and SH. At 20 km, Mt. Abu as well as Reunion Island show AO, which are stronger over Reunion Island. Interestingly, figure shows that SAO and QBO are exist in NH. SAO and QBO exist in SH but not significant at 95 % confidence interval. Except 50 and 60 km, both locations show AO. These oscillations are stronger in NH as compared to SH at 70–90 km. The QBO are dominant

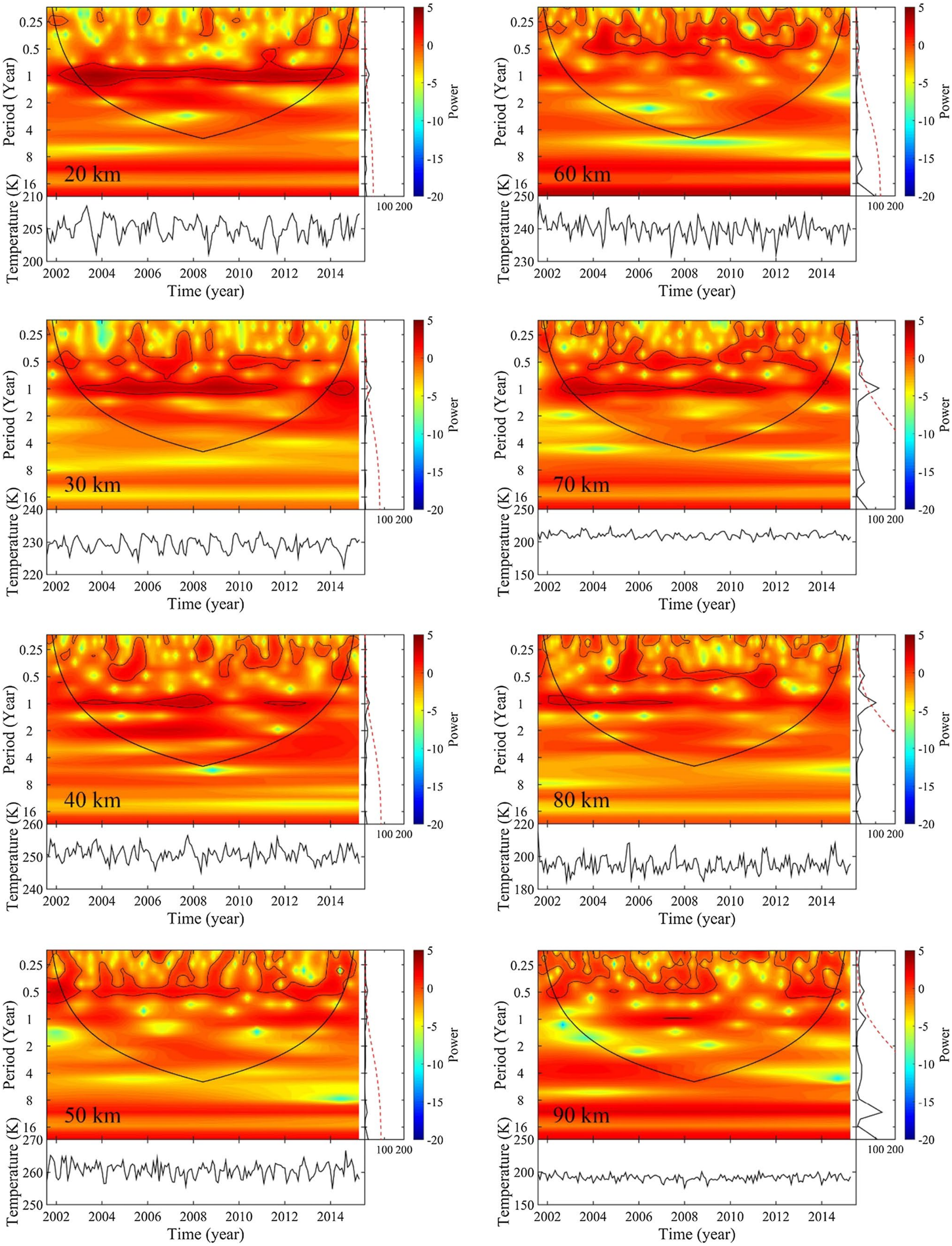

Fig. 10 Same as Fig. 9 but for Reunion Island

at altitude of 20–40 km over Mt. Abu region, whereas, these oscillations lie at 40 km over the SH (Fig. 8). Less than 6 months' oscillations are also observed in stratopause and lower mesosphere region. Overall, these results suggest that AO are dominated in both hemispheres as compared to SAO and QBO. The strength of AO is almost similar for both hemispheres in stratosphere, but more in upper mesosphere in NH. Contradictorily, SAO are stronger in SH as compared to NH. We also used every 1 km SABER temperature observations for oscillations studies using LSP from 20 to 90 km (figure not shown). It suggests that QBO are stronger in NH at 22 km. These oscillations also exist at 38 km but very less in amplitude for Reunion Island. The AO are not found in the range of 55–63 km in the NH, but the SH exhibits AO at these altitudes. Quarterly oscillations also exist in upper mesosphere in SH, which misses in NH.

Figures 9 and 10 show the wavelet transform at every 10 km from lower stratosphere to mesopause over Mt. Abu and Reunion Island respectively. Time series of SABER temperature observations are shown in lower panel, and upper panel shows corresponding wavelet spectra. The solid black line curve shows cone of influence and right panel shows power of oscillations and red dashed line shows confidence interval. Figure 9 and 10 show that AO are stronger at 20 km in both hemispheres at 95 % confidence interval. Mt. Abu shows SAO which are not very prominent in Reunion Island during selected time period. During year 2009, AO are not seen over Mt. Abu region at 20 km, however AO are significant in the SH for this period. Similar kind of oscillations are seen at 30 km in both the hemisphere, which also confirm by LSP analyses. Wavelet analyses also represent SAO and quarterly oscillations at this altitude which are not matches in the SH and NH. Wavelet spectra at 40 km shows AO and SAO at both selected locations, but QBO are seen significant over Mt. Abu region in the NH. Wavelet spectra very clearly demonstrate that AO are absent at 50 km in NH and SH and mainly dominated by less than annual periodicity. Similar features are also seen at 60 km, while SAO are noteworthy in SH as compared to NH at this altitude. In 70–90 km, Figs. 9 and 10 show that AO are significant at 70 km and these oscillations are not prominent at 90 km. We found a very interesting results for AO at 80 km, which shows that AO are significant mostly over Mt. Abu region but not dominated throughout the period in the SH at this altitude. However, SAO are more strength in southern region as compared to Mt. Abu. Overall, we found that both hemispheres are dominated by AO and SAO and these oscillations are different in nature at high altitudes (70 and 80 km).

4 Conclusions

In this study, two sub-tropical stations situated at Mt. Abu in the NH and Reunion Island in the SH are selected to distinguish the characteristics of middle atmosphere in different hemispheres. For this purpose, the SABER onboard TIMED satellite observations are used for thermal structure in stratosphere-mesosphere system during January 2002 to September 2015. Temporal variation of SABER observations in this period shows that stratopause temperature is warmer in Mt. Abu as compared to Reunion Island. Moreover, mean climatological behaviour of upper mesosphere shows that NH has higher temperature as compared to SH. Monthly climatology based on 14 years SABER observations shows that stratopause is warmer in NH, and cooler in upper mesosphere, as compared to SH. In general, stratosphere shows higher temperature over Mt. Abu compared to Reunion Island. The stratosphere sudden warming which are triggered from the NH Polar Regions and influence different latitudes depending upon their strength may be one of the reason for this anomalous behaviour. Monthly temperature anomaly shows that both hemisphere show identical temperature structure in stratosphere, with small positive anomaly at lower mesosphere in SH as compared to NH for the months of December to February. Mean temperature values during winter and summer season show that NH is warmer and cooler in summer and winter season respectively as compared to SH in stratosphere. Upper mesosphere shows a reverse nature. Three atmospheric models are also used to compare and contrast the vertical thermal structure for different months over both regions. Temperature simulated from these models matches well with SABER observations for lower stratosphere. Significant discrepancies are also seen in the mesospheric heights and differences are more pronounced over Reunion Island in the SH.

In addition to this, seasonal oscillations are studied using LSP and Wavelet transform techniques for stratosphere-mesosphere system which will help to distinguish the wave dynamics or wave features over these regions in the NH and SH. Results show that AO are stronger over Reunion Island at 20 km. The AO are found at both selected locations for all altitudes except 50 and 60 km. The QBO are dominant at 20–40 km over Mt. Abu region, and are exist at 40 km in SH. Overall, results suggest that AO are dominated in NH and SH as compared to SAO and QBO. The strength of AO is nearly similar in stratosphere, but strength of AO are more in NH as compared to SH in upper mesosphere. However, SAO are stronger in SH as compared to NH. Wavelet analyses found a very interesting results for AO at 80 km, which shows that AO are significant over Mt. Abu region, but are not dominated throughout the study period over the SH. However, SAO are more stronger in southern region.

Acknowledgments Authors are thankful to SABER onboard TIMED, CIRA-86, MSISE-90 and NRLMSIS-00 team members to provide valuable temperature data. This work is supported by Dept. of Space, Govt. of India.

References

Alexander MJ, Rosenlof KH (1996) Nonstationary gravity wave forcing of the stratospheric zonal mean wind. J Geophys Res 101(D18):23465–23474

Andrews DG (1989) Some comparisons between the middle atmosphere dynamics of the southern and northern hemispheres. Pure Appl Geophys. 130:213–232

Argall PS, Sica RJ (2007) A comparison of Rayleigh and sodium lidar temperature climatologies. Ann Geophys 25:27–35

Baldwin MP, Gray LJ, Dunkerton TJ, Hamilton K, Haynes PH, Randel WJ, Holton JR et al (2001) The quasi-biennial oscillation. Rev Geophys 39(2):179–229

Barnett JJ, Corney M (1985) Middle atmosphere reference model derived from satellite data. In: International council of scientific unions middle atmosphere program. Handbook for MAP, Vol. 16 p 47–85 (SEE N86-12814 03-46)

Batista PP, Clemesha BR, Simonich DM (2008) Tidal associated temperature disturbances observed at the middle atmosphere (30–65 km) by a Rayleigh LIDAR at 23o. Adv Space Res 41(9):1408–1414

Batista PP, Clemesha BR, Simonich DM (2009) A 14-year monthly climatology and trend in the 35–65 km altitude range from Rayleigh LIDAR temperature measurements at a low latitude station. J Atmos Sol–Terr Phys 71:1456–1462

Becker E, Müllemann A, Lübken FJ, Körnich H, Hoffmann P, Rapp M (2004) High Rossby-wave activity in austral winter 2002: Modulation of the general circulation of the MLT during the MaCWAVE/MIDAS northern summer program. Geophys Res Lett, 31(24

Bencherif H, Morel B, Moorgawa A, Michaelis M, Leveau J, Porteneuve J, Hauchecorne A, Faduilhe D (2000) Observation and first validation of stratospheric temperature profiles obtained by a Rayleigh-Mie LIDAR over Durban, South Africa. S Afr J Sci 96:487–492

Chandra H, Sharma Som, Acharya YB, Jayaraman A (2005) Rayleigh Lidar studies of thermal structure over Mt Abu. J Indian Geophys Un 9:279–298

Chanin, M.L., Hauchecorne, A., Smires, N., 1985. Contribution to the CIRA model from ground based lidar. MAP Handbook, vol. 16, pp. 305–314

Clancy RT, Rusch DW, Callan MT (1994) Temperature minima in the average thermal structure of the middle atmosphere (70–80 km) from analysis of 40- to 92-km SME global temperature profiles. J Geophys Res 99:19001–19020

Cooper M (2004) Validation of SABER temperature measurements using ground-based instruments. In: Proceedings of the IEEE international geoscience and remote sensing symposium, pp. 4099–4101

Croll J (1870) V.—The Boulder-clay of Caithness a Product of Land-ice. Geol Mag 7(71):209–214

Das U, Sinha HSS (2008) Long-term variations in oxygen green line emission over Kiso, Japan, from ground photometric observations using continuous wavelet transform. J Geophys Res Atmos, 113(D19)

Dou X, Tao L, Xu J, Liu H-L, Xue X, Wang S, Leblanc T, McDermid S, Hauchecorne A, Keeckhut P, Bencherif H, Heinselman C, Steinbrecht W, Mlynczak MG, Russell JM III (2009) Seasonal oscillations of middle atmosphere temperature observed by Rayleigh LIDARs and their comparisons with TIMED/SABER observations. J Geophys Res 114:D20103. doi:10.1029/2008JD011654

Farge M (1992) Wavelet transforms and their applications to turbulence. Annu Rev Fluid Mech 24(1):395–458

Forbes JM, Zhang X, Ward W, Talaat ER (2002) Climatological features of mesosphere and lower thermosphere stationary planetary waves within ± 40 latitude. J Geophys Res 107(D17):4322. doi:10.1029/2001JD001232

Fritts DC (1990) Gravity waves in the middle atmosphere of the southern hemisphere. In Dynamics, transport and photochemistry in the middle atmosphere of the southern hemisphere (pp. 171–189). Springer Netherlands

Fritts DC, Alexander MJ (2003) Gravity wave dynamics and effects in the middle atmosphere. Rev Geophys 41(1)

Fritts DC, Vanzandt TE (1993) Spectral estimates of gravity wave energy and momentum fluxes. Part I: energy dissipation, acceleration, and constraints. J Atmos Sci 50(22):3685–3694

Garcia RR, Dunkerton TJ, Lieberman RS, Vincent RA (1997) Climatology of the semiannual oscillation of the tropical middle atmosphere. J Geophys Res Atmos 102(D22):26019–26032

Gardner CS, Papen GC, Chu X, Pan W (2001) First Lidar observations of middle atmosphere temperatures, Fe densities, and polar mesospheric clouds over the North and South Poles. Geophys Res Lett 28:1199–1202

Gerding M, H€offner J, Lautenbach J, Rauthe M, L€ubken F-J (2008) Seasonal variation of nocturnal temperatures between 1 and 105 km altitude at 541 N observed by lidar. Atmos Chem Phys 8:7465–7482. doi:10.5194/acp-8-7465-2008

Giorgetta MA, Manzini E, Roeckner E (2002) Forcing of the quasi-biennial oscillation from a broad spectrum of atmospheric waves. Geophys Res Lett 29(8):1245. doi:10.1029/2002GL014756

Gobbi GP, Souprayen C, Congeduti F, Di Donfrancesco G, Adriani A, Viterbini M, Centurioni S (1995) Lidar observations of middle atmosphere temperature variability. In Annales Geophysicae (Vol. 13, No. 6, pp. 648–655). Springer-Verlag

Gray LJ, Beer J, Geller M, Haigh JD, Lockwood M, Matthes K, Cubasch et al. (2010). Solar influences on climate. Rev Geophys 48(4)

Gross MR, McGee TJ, Ferrare RA, Singh U, Kimvilikani P (1997) Temperature measurements made with a combined Rayleigh–Mie/Raman Lidar. Appl Opt 24:5987–5995

Hartmann DL, Mechoso CR, Yimazaki K (1984) Observations of wave-mean flow interaction in the Southern Hemisphere. J Atmos Sci 41:351–362

Hauchecorne A, Chanin ML, Keckhut P (1991) Climatology and trends of the middle atmospheric temperature (33–87 km) as seen by Rayleigh lidar over the south of France. J Geophys Res Atmos 96(D8):15297–15309

Hauchecorne A, Chanin ML, Keckhut P, Nedeljkovic D (1992) Lidar monitoring of the temperature in the middle and lower atmosphere. Appl Phys B 54:2573–2579

Hirota I, Hirooka T, Shiotani M (1983) Upper stratospheric circulations in the two hemispheres observed by satellites. Q J R Meteorol Soc 109:443–453

Jenkins DB, Wareing DP, Thomas L, Vaughan G (1987) Upper stratospheric and mesospheric temperatures derived from lidar observations at Aberystwyth. J Atmos Terr Phys 49:287–298

Kang SM, Seager R, Frierson DM, Liu X (2013) Croll revisited: why is the northern hemisphere warmer than the southern hemisphere? Clim Dyn 44(5–6):1457–1472

Karlsson B, McLandress C, Shepherd TG (2009) Inter-hemispheric mesospheric coupling in a comprehensive middle atmosphere model. J Atmos Solar Terr Phys 71(3):518–530

Kishore Kumar G, Venkat Ratnam M, Patra AK, Vijaya Bhaskara Rao S, Russell J (2008) Mean thermal structure of the low-latitude middle atmosphere studied using Gadanki Rayleigh lidar, Rocket, and SABER/TIMED observations. J Geophys Res 113:D23106. doi:10.1029/2008JD010511

Kornich H, Becker E (2010) A simple model for the interhemispheric coupling of the middle atmosphere circulation. Adv Space Res 45(5):661–668

Lal S, Subbaraya BH, Narayanan V (1979) Equatorial stratospheric and meso-spheric structural variations during the years 1971–74, 1979. Sp Res 19:147–157

Leblanc T, McDermid IS, Keckhut P, Hauchecorne A, She C, Krueger DA (1998) Temperature climatology of the middle atmosphere from long-term lidar measurements at middle and low latitudes. J Geophys Res 103:17191–17204

Li T, Leblanc T, McDermid IS (2008) Interannual variations of middle atmospheric temperature as measured by the JPL lidar at Mauna Loa Observatory, Hawaii (19.51 N, 155.61 W). J Geophys Res 113:D14109. doi:10.1029/2007JD009764

Lomb NR (1976) Least-squares frequency analysis of unequally spaced data. Astrophys Space Sci 39(2):447–462

Matthes K, Kodera K, Garcia RR, Kuroda Y, Marsh DR, Labitzke K (2013) The importance of time-varying forcing for QBO modulation of the atmospheric 11 year solar cycle signal. J Geophys Res Atmos 118(10):4435–4447

Mechoso CR, Hartmann DL, Farrara JD (1985) Climatology and interannual variability of wave, mean-flow interaction in the Southern Hemisphere. J Atmos Sci 42(20):2189–2206

Mertens CJ, Mlynczak MG, Lopez-Puertas M, Wintersteiner PP, Picard RH, Winick JR, Gordley LL, Russell JM III (2001) Retrieval of mesospheric and lower thermospheric kinetic temperature from measurements of CO2 15-mm Earth limb emission under non-LTE conditions. Geophys Res Lett 28(1391–1394):2000G. doi:10.1029/L012189

Mertens CJ, Russell JM III, Mlynczak MG, She CY, Schmidlin FJ, Goldberg RA et al (2009) Kinetic temperature and carbon dioxide from broadband infrared limb emission measurements taken from the TIMED/SABER instrument. Adv Space Res 43(1):15–27

Mohankumar K (1994) Temperature variability over the tropical middle atmosphere. Ann Geophys 12:448–496

Morel B, Bencherif H, Keckhut P, Baldy S, Hauchecorne A (2002) Evidence of tidal perturbations in the middle atmosphere over Southern Tropics as deduced from LIDAR data analysis. J Atmos Solar Terr Phys 64:1979–1988

Namboothiri SP, Sugimoto N, Nakane H, Matsui I, Murayama Y (1999) Rayleigh lidar observations of temperature over Tsukuba, winter thermal structure and comparison studies. Earth, Planets Sp 51:825–832

Nee JB, Thulasiramana S, Chen WN, Venkat Ratnam M, Narayana Rao D (2002) Middle atmospheric temperature structure over two tropical locations, Chung–Li (251 N, 1211E) and Gadanki (13.51 N,79.21E). J Atmos Solar Terr Phys 64:1311–1319

Parameswaran K, Sasi MN, Ramkumar G, Nair PR, Deepaa V, Krishnamurthy BV, Prabhakaran Nayar SR, Revathy K, Mrudula G, Satheesan K, Bhavanikumar Y, Sivakumar V, Raghunath K, Rajendraprasad T, Krishnaiah M (2000) Altitude profiles of temperature from 4–80 km over the tropics from MST radar and lidar. J Atmos Sol–Terr Phys 62:1327–1337

Philander SGH, Gu D, Lambert G, Li T, Halpern D, Lau NC, Pacanowski RC (1996) Why the ITCZ is mostly north of the equator. J Clim 9(12):2958–2972

Pulido M, Thuburn J (2008) The seasonal cycle of gravity wave drag in the middle atmosphere. J Clim 21:4664–4679

Randel W, Udelhofen P, Fleming E, Geller M, Gelman M, Hamilton K, Karoly Ortland D, Pawson S, Swinbank R, Wu F, Baldwin M, Chanin ML, Keckhut P, Labitzke K, Remsberg E, Simmons A, Wu D (2004) The SPARC intercomparison of middle atmospheric climatologies. J Clim 17:986–1003

Remsberg EE, Bhatt PB, Deaver LE (2002) An assessment of the Quality of HALOE temperature profiles in the mesosphere with Rayleigh Backscatter Lidar and inflatable falling sphere measurements. J Geophys Res 107(D19):4411. doi:10.1029/2001JD001366

Remsberg EE, Marshall BT, Garcia-Comas M, Krueger D, Lingenfelser GS, Martin-Torres et al. (2008). Assessment of the quality of the Version 1.07 temperature-versus-pressure profiles of the middle atmosphere from TIMED/SABER. J Geophys Res Atmos, 113(D17)

Sasi MN (1994) A reference atmosphere for the Indian equatorial zone. Indian J Radio Space Phys 23:299–312

Sasi MN, Sengupta K (1979) A model equatorial atmosphere over the Indian zone from 0 to 80 km. Scientific Report ISRO-VSSC-SR-19

Sato K, Watanabe S, Kawatani Y, Tomikawa Y, Miyazaki K, Takahashi M (2009) On the origins of mesospheric gravity waves. Geophys Res Lett 36:L19801. doi:10.1029/2009GL039908

Sato K, Tateno S, Watanabe S, Kawatani Y (2012) Gravity wave characteristics in the Southern Hemisphere revealed by a high-resolution middle-atmosphere general circulation model. J Atmos Sci 69(4):1378–1396

Scargle JD (1982) Studies in astronomical time series analysis. II-Statistical aspects of spectral analysis of unevenly spaced data. Astrophys J 263:835–853

Sharma S, Sivakumar V, Bencherief H, Chandra H, Rao PB, Rao DN (2006) A comprehensive study on middle atmospheric thermal structure over a low and near mid-latitude stations. Adv Sp Res 37:2278–2283

Sharma S, Sridharan S, Chandra H, Lal S, Acharya YB (2012) Middle atmospheric thermal structure over sub-tropical and tropical Indian locations using Rayleigh lidar. Planet Sp Sci 63:36–48

Sharma S, Chandra H, Lal S, Acharya YB, Jayaraman A, Gadhavi H, Sridharan S, Chandra S (2015) Study of thermal structure differences from coordinated lidar observations over Mt. Abu (24.5° N, 72.7° E) and Gadanki (13.5° N, 79.2° E). Earth, Planets Sp 67(1):1–11

Shiotani M, Hirota I (1985) Planetary wave-mean flow interaction in the stratosphere: a comparison between Northern and Southern Hemispheres. Q J R Meteorol Soc 111:309–334

Sica RJ, Izawa MRM, Walker KA, Boone C, Petelina SV, Argall PS, Bernath P, Burns GB, Catoire V, Collins RL, Daffer WH, Clercq C De, Fan ZY, Firanski BJ, French WJR, Gerard P, Gerding M, Granville J, Innis JL, Keckhut P, Kerzenmacher T, Klekociuk AR, Kyro E, Lambert JC, Llewellyn Manney GL, McDermid IS, Mizutani K, Murayama Y, Piccolo C, Raspollini P, Ridolfi M, Robert C, Steinbrecht W, Strawbridge KB, Strong K, Stubi R, Thurairajah B (2008) Validation of the atmospheric chemistry experiment (ACE) Version 2.2 temperature using ground-based and space-borne measurements. Atmos Chem Phys 8:35–62

Sivakumar V, Rao PB, Krishnaiah M (2003) Lidar measurements of stratosphere–mesosphere thermal structure at a low latitude: comparison with satellite data and models. J Geophys Res 108(D11):4342. doi:10.1029/2002JD003029

Sivakumar V, Prasanth PV, Kishore P, Bencherif H, Keckhut P (2011) Rayleigh Lidar and Satelite (HALOE, SABER, CHAMP and COSMIC) measurements of stratopshere–mesosphere temperature over southern sub-tropical site, Reunion (20.81S, 55.51E): climatology and comparison study. Ann Geo Phys 29:649–662

Whiteway JA, Carswell AI (1994) Rayleigh lidar observations of thermal structure and gravity wave activity in the high arctic during a stratospheric warming. J Atmos Sci 51:3122–3136